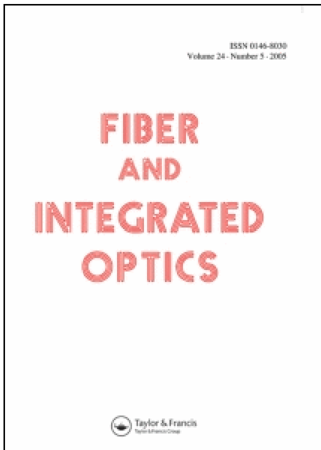

Fiber and Integrated Optics
Publication details, including instructions for authors and subscription information:
http://www.informaworld.com/smpp/title~content=t713771194

Optical Fiber Sensor Technology in Portugal

A. B. Lobo Ribeiro [a]; J. L. Santos [bc]; J. M. Baptista [cd]; L. A. Ferreira [c]; F. M. Araújo [c]; A. P. Leite [b]
[a] Universidade Fernando Pessoa, Porto, Portugal
[b] Universidade do Porto, Porto, Portugal
[c] INESC-Porto, Porto, Portugal
[d] Instituto Superior de Engenharia do Porto, Porto, Portugal

Online Publication Date: 01 May 2005

To cite this Article: Ribeiro, A. B. Lobo, Santos, J. L., Baptista, J. M., Ferreira, L. A., Araújo, F. M. and Leite, A. P. (2005) 'Optical Fiber Sensor Technology in Portugal', Fiber and Integrated Optics, 24:3, 171 — 199

To link to this article: DOI: 10.1080/01468030590922722
URL: http://dx.doi.org/10.1080/01468030590922722

Fiber and Integrated Optics, 24:171–199, 2005

ISSN: 0146-8030 print/1096-4681 online
DOI: 10.1080/01468030590922722

Optical Fiber Sensor Technology in Portugal

A. B. LOBO RIBEIRO

Universidade Fernando Pessoa
Porto, Portugal

J. L. SANTOS

Universidade do Porto
Porto, Portugal, and
INESC-Porto
Porto, Portugal

J. M. BAPTISTA

INESC-Porto
Porto, Portugal, and
Instituto Superior de Engenharia do Porto
Porto, Portugal

L. A. FERREIRA
F. M. ARAÚJO

INESC-Porto
Porto, Portugal

A. P. LEITE

Universidade do Porto
Porto, Portugal

A general overview of the R&D activity in fiber optic sensing developed over the last fifteen years in Portugal is given. Different topics are addressed, including interferometric, intensity and Bragg grating based fiber optic sensors, signal processing and multiplexing techniques, optical current sensors, together with some references to field trials and applications. Possible guidelines for present and future national R&D activity on this subject are outlined.

Keywords fiber optic sensor, interferometric sensors, fiber Bragg gratings, optical current sensors, optical sensor multiplexing, intensity optical sensors

Introduction

Optical fiber sensors may be defined as devices through which a physical, chemical, biological, or other measurand interacts with light, either guided in an optical fiber (intrinsic sensor) or guided to an interaction region (extrinsic sensor) by an optical fiber, to produce an optical signal related to the parameter of interest. Fiber sensors can be designed so that the measurand interacts with one or several optical parameters of the guided light (intensity, phase, polarization, wavelength). Independently of the sensor type, the light modulation must be processed into an optical intensity signal at the receiver, which subsequently performs a conversion into an electric signal. In general, the main

Accepted 4 March 2005.
Address correspondence to A. B. Lobo Ribeiro, Faculdade Ciências da Saúde, Universidade Fernando Pessoa, Rua Carlos Maia 296, Porto 4200-150, Portugal. E-mail: alobo@ufp.pt

interest in this type of sensor comes from the fact that the optical fiber itself offers numerous operational benefits. It is electromagnetically passive, so it can operate in high and variable electric field environments (like those typical of the electric power industry); it is chemically and biologically inert, since the basic transduction material (silica) is resistant to by most chemical and biological agents; and its packaging can be physically small and lightweight. Taking advantage of the intrinsic low optical attenuation of the fiber, it is possible to attain distributed sensing, where the measurand can be determined as a function of the position along the length of the fiber simply by interrogating the fiber from one end. Also, the optical fiber can be operated over very long transmission lengths, so that the sensor can easily be placed kilometers away from the monitoring station and data can be reliably transmitted between the two. It is also possible to perform multiplexed measurements using large arrays of remote sensors, operated from a single optical source and detection unit, with no active optoelectronic components located in the measurement area, thereby retaining electromagnetic passiveness and environmental resistance [1].

In Portugal, the activity in fiber optic sensing started by the end of eighties, benefiting from a strategic collaboration between the University of Porto/INESC Porto and the Applied Optics Group of the Physics Department of University of Kent, U.K., which was extended later to the Department of Physics and Optical Science of University of North Carolina at Charlotte. Due to that, and over the last fifteen years, those Portuguese institutions essentially framed the country activity in this field. More recently, the University of Aveiro has been also engaged in fiber sensing R&D, particularly in fiber Bragg grating–based sensors.

This article summarizes some of the results arising from the fiber-sensing activity developed in the country over that period. It is organized in the following sections: interferometric fiber optic sensors; intensity-based fiber sensors; fiber Bragg gratings: interrogation and simultaneous measurement; optical current sensors; sensor multiplexing; reference to some field trials and applications; and, to conclude, some present and future trends. When considered necessary, the research presented is preceded by a short introduction with selected bibliographic references that give some insight into its development environment.

Interferometric Sensors

The single-mode fiber permits retention of the coherence properties of the radiation that propagates along the fiber, a feature that opened the opportunity for the implementation of fiber sensors based on phase modulation. Almost all physical measurands introduce modifications to the phase of the propagated light. If the effect is too small to be directly detected, the design of an adequate interface between the fiber and the measurand will increase signal coupling by several orders of magnitude. In the context of optical fiber sensors, and not considering fiber Bragg grating–based sensors, it is the domain of phase (interferometric) sensors where the largest investments occurred, both in terms of basic research and prototype design. The main reason for this effort stays with the extremely high sensitivities that these sensors can offer [2].

This high performance level also motivated the research of this type of sensors in Portugal, particularly in what concerns the development of techniques for their interrogation and multiplexing. The analysis of particular intererometric sensing structures, such as the low-finesse Fabry-Pérot interferometer (LFFPI), was also developed. In many potential applications, the requirement of small sensor heads to perform sensitive point measurements is the main decision criteria. Before the appearance of fiber Bragg gratings, the LFFPI structure with a short optical cavity was the only attractive choice for the basic sensing element. Such interferometers exploit the cleaved distal endface of the optical fiber as one interface and an external reflecting surface as the other, or alternatively, the two air-glass interfaces of a length of optical fiber can be used. The LFFPI offers the advantages of being simple and compact, providing high measurand sensitivity, and also being lead insensitive because any environmental fluctuations that affect the optical phase or the light polarization along the optical fiber system are common to the interfering optical fields.

To extract the measurand information it is necessary to recover the Fabry-Pérot (FP) interferometric phase. For this sensing configuration, the set of signal processing techniques used for other interferometric topologies is reduced because of the small path imbalance of the FP structure, which very often limits the utilization of active homodyne and synthetic heterodyne processing schemes. Due to that, many configurations for FP interferometric reading based on the generation of two quadrature phase-shifted signals have been reported [3–8]. The starting point of all these signal processing techniques is the assumption that the transfer function of the FP can be approximated by that of the two-wave interference case, which is indeed obtained in the limit of small power reflectivity of the cavity optical interfaces. When this situation does not occur, a certain level of phase reading error is introduced. A study of this effect was reported in Santos et al. [9], and the main result is summarized in Figure 1. For the case of air–glass interfaces, the maximum deviation is $\approx 5\%$, but the main problem is that this deviation changes with the interferometer phase, making the implementation of compensation procedures difficult.

Another largely considered approach to address remote FP cavities is coherence reading (white light interferometry). Here, the length L of the cavity is much larger than the coherence length of the optical source, L_c. To address the cavity, a receiving interferometer with a path imbalance tuned to $2L$ is utilized. In this case, it can be shown that coherence processing always generates a two-beam transfer function, even in the situation where R is not small [9]. The white light technique can not only be used to address the FP interferometer, but also to interrogate it through dynamic implementation of the zero path imbalance condition for the two interferometers set. Alternatively, if this combined path imbalanced is kept within the coherence length of the optical source, then

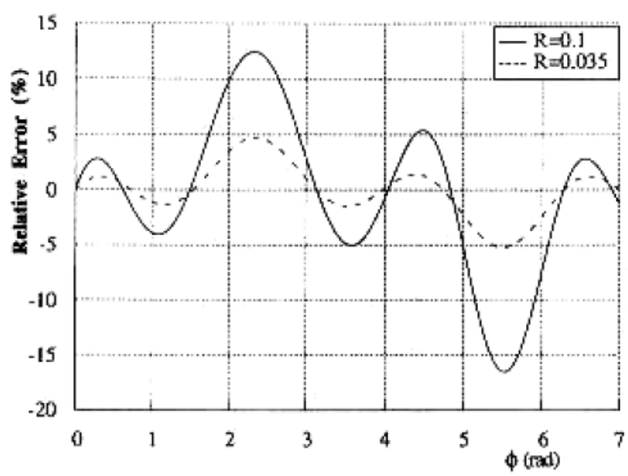

Figure 1. Scale error (relative to the two-beam limit) introduced by applying the two quadrature phase-shifted techniques to the FP transfer function (from [8]).

it is possible to recover without error the interferometer phase using the two quadrature components technique.

Fiber Bragg gratings (FBG) are remarkable sensing elements [10]. In addition, they allow the additional flexibility to implement signal processing techniques for interferometric demodulation, and such characteristic triggered local research oriented to the interrogation of FP interferometers. An example of that work was reported in Dahlem et al. [11], where FBGs were used as spectral discriminators to interrogate remote FP cavities through the generation of two quadrature phase-shifted signals (Figure 2). The two FBGs used had resonant wavelengths of $\lambda_{B1} = 1551.1$ nm and $\lambda_{B2} = 1556.9$ nm (0.2-nm bandwidth), and the cavity path imbalance was tuned to introduce a differential phase shift of $3\pi/2$ between the two interferometric signals at detectors D_1 and D_2. Using this signal processing technique and for the case of mirror displacement measurement, a resolution of $\sim$90 pm/$\sqrt{\text{Hz}}$ was achieved. For temperature measurement, the resolution turned out to be $\sim$0.05°C/$\sqrt{\text{Hz}}$.

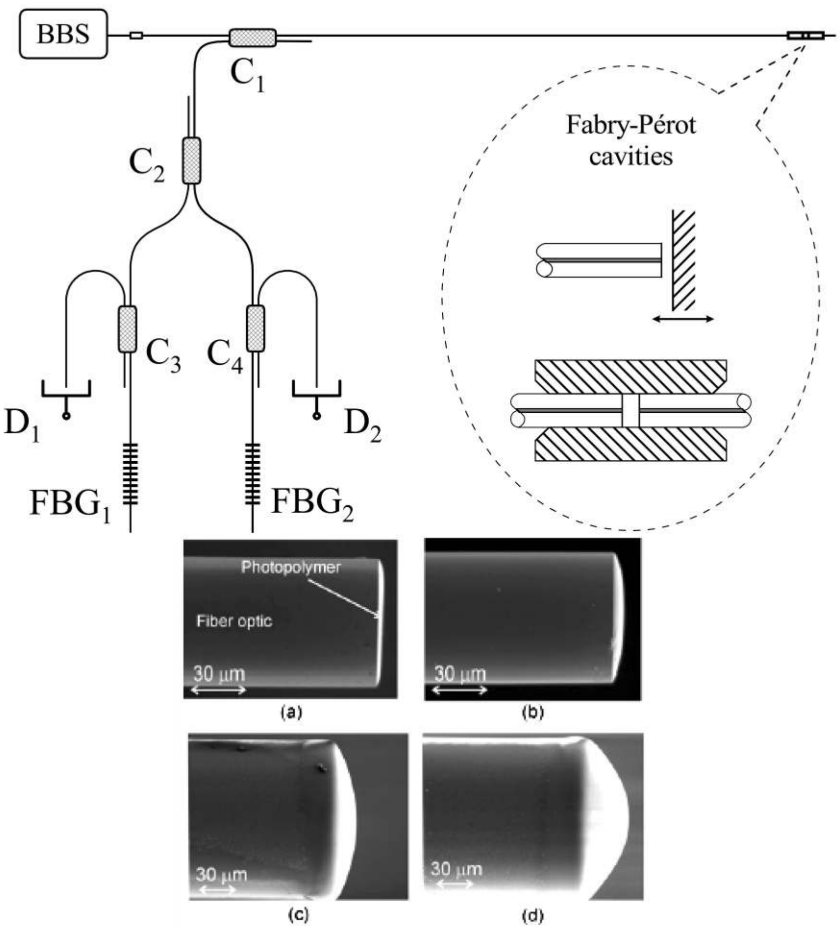

Figure 2. Experimental setup for FBGs based generation of quadrature phase-shifted signals for interrogation of remote Fabry-Perot interferometers (from [11]). Bottom: SEM photos of photopolymer fiber tips fabricated with different widths: ≈5 μm (a); ≈10 μm (b); ≈22 μm (c); ≈35 μm (d) (from [12]).

This technique was used to interrogate an FP interferometer based on photopolymer growth [12]. The photopolymer microcavity was grown on the tip of a single-mode fiber by the dip-coating technique. Figure 2 also shows SEM images of photopolymer fiber tips fabricated with different numbers of immersions. For the case of the photopolymer cavity with $\approx$10 μm width, a temperature phase sensitivity of $\approx$15°C was found. Admitting a modest phase resolution of 1 mrad, this corresponds to a temperature resolution of $\approx$67 μ°C, which is illustrative of the sensitivities that can be achieved with these materials and the processing technique described.

Another developed approach to interrogate remote FP interferometers relied on the modulation of the transfer function of a wavelength division multiplexer (WDM). The basic concept is illustrated in Figure 3 [13]. An analysis of the configuration obtains, in the situation where the spectral period of the WDM is similar to the one of the FP interferometer,

$$V_o = G \cos\lfloor 2C|_{\lambda_0} d + \phi \rfloor, \qquad \phi = \frac{4\pi n L}{\lambda_0} \tag{1}$$

where G is a constant, d is the interaction length of the WDM coupler, and $C|_{\lambda_0}$ is its coupling coefficient evaluated at λ_0, the central wavelength of the radiation that illuminates the interferometer. This equation shows that modulation of the length d by a signal $s(t)$ makes it possible to recover the phase ϕ, utilizing any of the signal processing techniques developed along the years for interferometric phase retrieval. In the reference cited, the authors opted to generate an electric carrier by sawtooth or sinusoidal modulation of the WDM interaction length. For the first modulation format, an FP displacement sensitivity of $\approx$0.2 nm/$\sqrt{\text{Hz}}$ was achieved.

The noise (and scale error) caused by fluctuations in the polarization states of the interfering waves (polarization-induced fading) has been pointed out from the beginning as one of the limiting factors determining the performance of these interferometric systems [14]. Many researchers have studied the implications of changes in the input state of polarization (SOP) on both the visibility and phase of fiber optic interferometers [15],

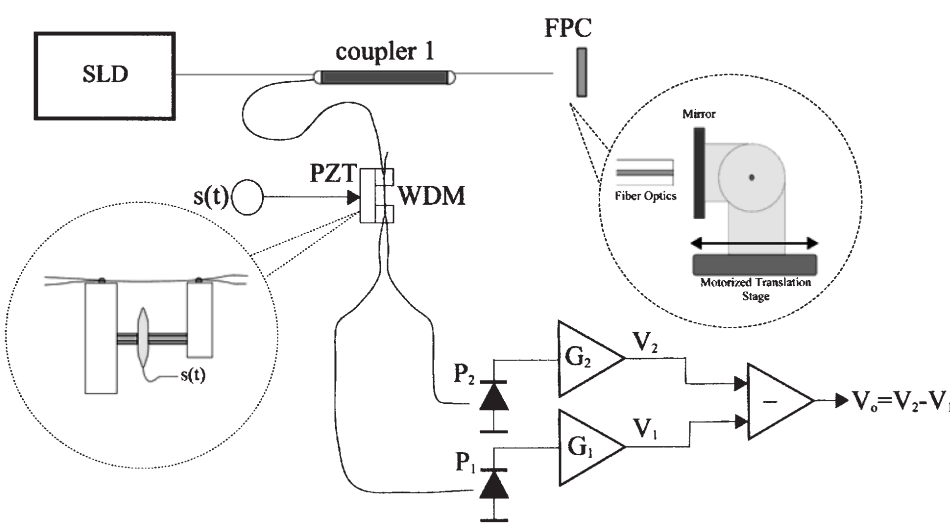

Figure 3. Interrogation of a Fabry-Pérot interferometer using a tuneable WDM (from [13]).

and several ingenious schemes have been considered to overcome these effects [16, 17]. However, it was only after the advent of Faraday rotator mirrors (FRM) that effective solutions became available [18, 19].

In this context, it was commonly believed that environmental perturbations on the fiber linking two tandem interferometers in white light systems had no effect on the global performance of the system. However, a study published in 1994 showed that both the phase and the amplitude of the output signals are significantly affected by external induced birefringence in the downlead fiber and, in some cases, this may cause total fading of the interference signal [20]. The experiment shown in Figure 4 illustrates this phenomenon and demonstrated a technique to overcome it [21]. In the white light sensing system shown, the sensing interferometer is a fiber Michelson interferometer and the processing interferometer is a conventional Mach-Zehnder. The system is considered balanced to within the coherence length of the input light. PZT 2 is used to induce a sinusoidal phase signal at 1 kHz in the sensing interferometer. A 40-Hz sinusoidal voltage signal was applied to PZT1 to simulate the environmental perturbation in the fiber lead. Figure 4 (right top) shows the spectrum of the signal from output 2 of the tandem configuration without the FRMs. Two strong sidebands appear in this figure, which are produced by the modulation applied to the fiber lead. It is obvious that these sidebands can not be distinguished from a signal with the same frequency, if such signal was applied to the sensing interferometer. In the same figure (right down) the signal obtained from the same output, but now with the FRMs introduced in the system can be observed. The action of these devices in suppressing the lead-induced signal is clear, which shows the effectiveness of this technique. Here, it is worthwhile to note that this conclusion stands on the assumption that the polarization state of the light does not change in the coupling region of the fiber directional couplers. If that happens (which can occur in certain conditions), this effectiveness is degraded to a certain degree [22].

Intensity Based Sensors

Optical fiber intensity sensors are very attractive since they are conceptually simple, reliable, small-sized, and suitable for a wide range of applications at low cost. However, to ensure accurate measurements, the implementation of a reference channel is vital. Such channel should provide insensitivity to source intensity fluctuations and to variable optical transmission losses in the fiber link, couplers, and connectors, which are often indistinguishable from transducer-caused effects [23]. In this context, a self-referencing signal processing scheme is required in order to have a robust and precise fiber optic intensity sensor.

Baptista et al. [24–27] studied various frequency-based self-referenced fiber optic intensity sensors implemented with different configurations, namely the recirculating loop, Mach-Zehnder, Michelson, and Sagnac. As an example, Figure 5 presents a Michelson topology with optical feedback. The frequency response of such structures, when the input optical power is modulated at a particular frequency, shows that for some frequencies the amplitude of the output optical power waveform is maximum (constructive interference frequencies, f_I), while for other frequencies it results in a minimum value for that amplitude (off-constructive interference frequencies, f_{OI}).

The theoretical and experimental transfer functions for the Michelson topology with optical feedback are illustrated in Figure 6a, b, and c. The parameter g indicates the optical power attenuation factor externally induced in the fiber structure. For $g = 1$, the configuration is power balanced and there is no induced optical loss, while for $g = 0$

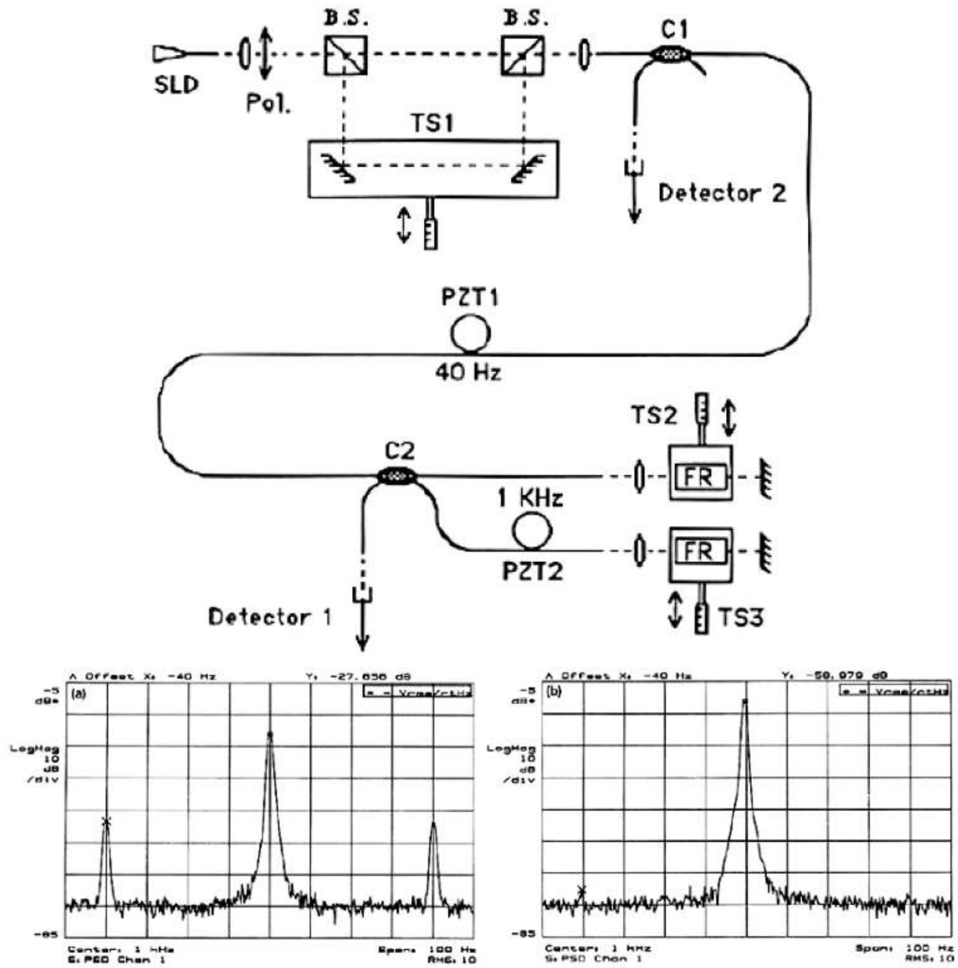

Figure 4. Scheme of the experimental arrangement used to test the lead sensitivity in a white light sensing system using Faraday rotators mirrors (FRM) to eliminate this effect. Signal at detector 2 without (bottom left) and with (bottom right) FRMs (from [21]).

all light is lost in the sensing arm. It can be seen that when the induced loss rises, in other words when g gets closer to zero, the difference between peaks and valleys shortens until the frequency response becomes constant. On the other hand, when no external losses are induced in the fiber interferometer ($g = 1$), the differences between peaks and valleys are at their maximum. The ratio of the value of the transfer function at an off-constructive interference frequency to its value at a constructive interference frequency (R parameter) depends only on the optical losses inside the fiber sensing structure (intrinsic and induced losses) and is not influenced by optical power fluctuations that can occur outside the sensing head. Therefore, the modulation of the R parameter provides a self-referencing scheme that makes the measurand read-out independent of possible unwanted light intensity modulation along the optical system.

An experimental result for the R parameter is shown in Figure 6d. In this case, the sensor includes a microbend optical fiber sensing head embedded in carbon fiber

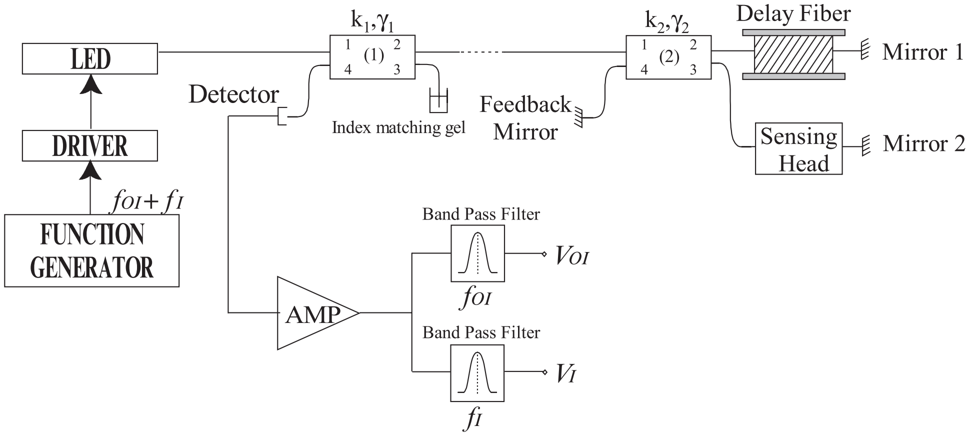

Figure 5. Block diagram of the intensity-based fiber optic sensing configuration using a Michelson topology with optical feedback (from [26]).

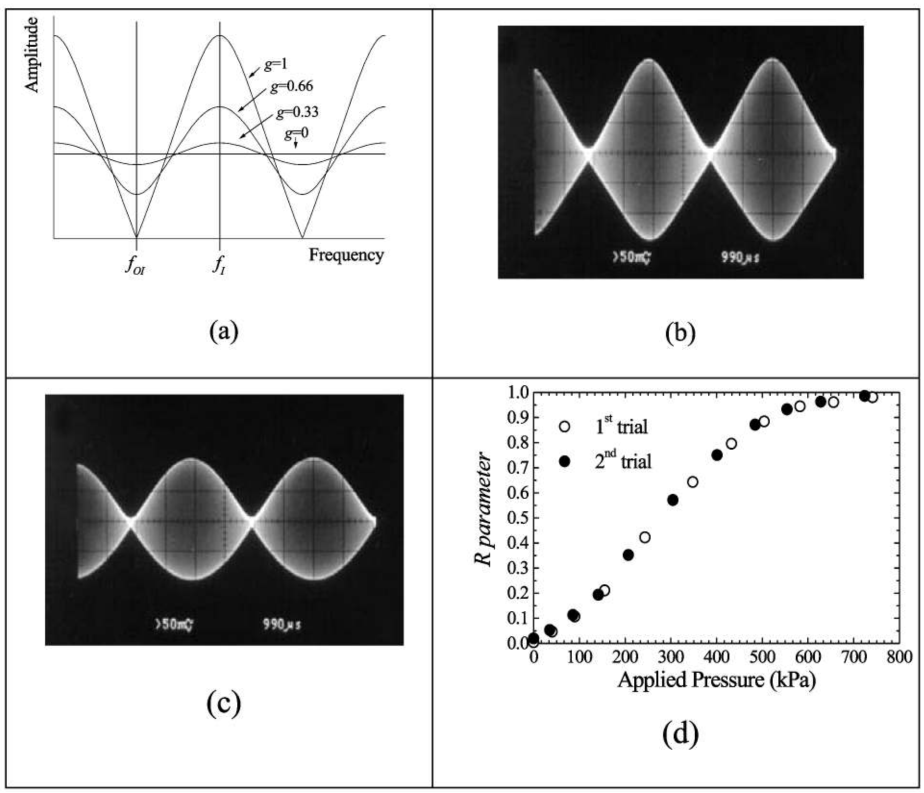

Figure 6. Transfer function of the Michelson configuration with optical feedback: theoretical (a); experimental for $g = 1$ (b); experimental for $g < 1$ (c); experimental results of the R parameter versus applied pressure (d) (from [26] and [28]).

reinforced plastic, which acts as a load cell for structural monitoring in civil engineering. To analyze the self-referencing properties of the sensor, the optical intensity of the source was decreased down to 75% of its nominal value during the second trial. As can be seen, the system immunity to optical power fluctuations is effective [28].

Cavaleiro et al. [29] proposed a referencing concept for intensity sensors based on the use of fiber Bragg gratings (FBGs). As shown in Figure 7, the intensity sensor is designed as a reflective cavity for primary displacement measurement. It uses two identical FBGs, one in the sensor head and the other in the processing region. The optical power at the Bragg wavelength (BW) is reflected by the grating in the sensing head and provides the referencing signal. All the other input spectral power is transmitted by the grating and is modulated by the measurand. After reflection in the mirror at distance d, a fraction of this power is reinjected in the lead fiber. The discrimination of the sensing and referencing optical powers is performed in wavelength by using a second FBG, as indicated in the figure. When this grating (FBG_R) is prestrained in such a way that the gratings spectral signatures coincide, the ratio between the signals V_1 and V_2 is independent of the optical power I_0 injected in the input fiber, as well as of any other power fluctuation along the common path of the sensing and referencing signals. Figure 7 also shows the transfer function of the intensity sensor without and with reference signal. This referencing technique is independent of the structure of the sensing head, the only requirement being that it must be of reflective type. Additionally, the variations of voltage V_{lock} in Figure 7a are proportional to the temperature variations of the sensing head.

Abad et al. [30] demonstrated another FBG-based referencing concept for intensity sensors. The optical power into the system is sinusoidally modulated at a particular frequency. Two signals are obtained from the sensing head. The first one comes from the reflection of an FBG located before the transducer that operates at a certain wavelength. Therefore, this signal is not affected by the measurand. The second signal is obtained from another FBG with a slightly different resonance wavelength, located after the transduction and thus containing the measurand information. Considering that there is no optical interference present in the system, since spectral overlap is absent, only electrical beating of these two signals can be expected at detection. The phase of this beating signal is only dependent on the measurand-induced loss in the sensing head, being independent of any other losses along the system. With this technique, the system response has been demonstrated to be almost unaffected by network power variations as high as 90% of the total power launched by the source.

Fiber Bragg Gratings

Fiber Bragg gratings (FBGs) are simple, versatile, and small intrinsic sensing elements that can be written in silica fibers and which consequently have all the advantages normally attributed to fiber sensors [10]. In addition, due to the fact that the measurand information is encoded in the resonant wavelength of the structure, which is an absolute parameter, these devices are inherently self-referenced and can be easily multiplexed, which is particularly important in the context of distributed sensing. All these characteristics triggered a research burst by the mid-nineties, addressing diversified topics like the fundamentals of UV-induced refractive index modulation of the fiber core, interrogation of these wavelength encoded devices, new sensing head concepts integrating FBGs, including their multiplexing, and applications. In Portugal the first FBGs were fabricated in 1994, and since then significant R&D activity has been polarized around these devices, both in fiber sensing and in communication. Previous sections already identified

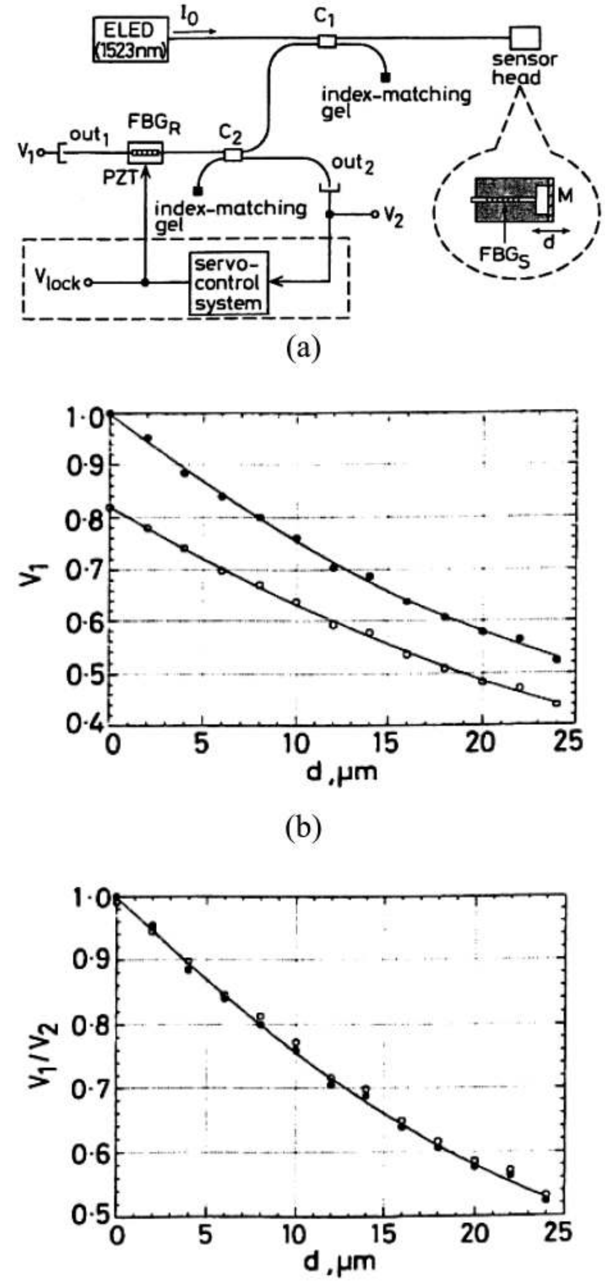

Figure 7. Experimental setup of the self-referenced fiber optic intensity sensor based on the utilization of fiber Bragg gratings (a). Transfer functions of the sensor without (b) and with referenting (c) (from [29]).

the utilization of these structures in referencing concepts for intensity based sensors. Results of the more basic work by Araújo et al. on the photosensitivy mechanisms responsible for the UV induced imprint of the refractive index modulation pattern can be found in [31]. In this section, the topics addressed are limited to FBG interrogation and application of these devices to the problem of simultaneous measurement of two or more measurands.

Interrogation

Several general concepts were explored for FBG interrogation. One of them was spectral filtering, which was achieved by utilization of a biconical fiber filter [32], using the spectral slope of SLD based optical sources (which permitted a minimum configuration for FBG interrogation [33]). This provided the combination of spectral filtering with amplitude-to-phase optical conversion [34] and used a chirped grating written in an erbium-doped fiber (which permits tuning of the FBG readout sensitivity; Romero et al. [35]. Another approach was based on the utilization of matched gratings with homodyne [36] or heterodyne detection [37]. Interferometric interrogation was also investigated by Jorge et al. [38]. The spectral modulation properties of multimode laser diodes [39–41, 42], as well as of wavelength division fiber couplers [43, 44], were also explored in the context of FBG interrogation.

Figure 8 shows the experimental set-up implemented to test the FBG interrogation concept based on the modulation of a multimode laser diode [39]. It relies on the generation of an electric carrier by using a modulated multimode laser diode to illuminate the FBG. The change in Bragg wavelength is measured by tracking the phase of the carrier at the detector output, either in an open- or closed-loop configuration. A pigtailed multimode laser diode operating at 1318 nm (wavelength of the central mode) was used to illuminate the FBG in the spectral position of one of the laser lateral modes. By modulating the injection current, the laser wavelength was modulated by a sawtooth signal at 1 kHz. Figure 8 also shows the output signal as seen in the scope. Since the laser line spectral width is much smaller than the grating spectral width, sweeping the grating spectrum with the laser mode reveals the spectral structure of the fiber grating. The demodulation principle is also illustrated in the same figure, which displays the change in the output signal when the system is operated in open loop and the strain applied to the grating changes by $\delta\varepsilon = 233\ \mu\varepsilon$.

The closed-loop format is set when the switch in the figure is closed, in which case the change in Bragg wavelength is measured by monitoring the laser bias current. In this mode of operation, the system response to applied strain and temperature is given in the bottom of Figure 8. From the data spread and the bandwidth of the feedback loop ($\approx$20 Hz), resolutions of $0.05°\text{C}/\sqrt{\text{Hz}}$ and $0.7\ \mu\varepsilon/\sqrt{\text{Hz}}$ were achieved.

Figure 9 addresses another concept for FBG interrogation based on active control of the spectral response of a fused biconical wavelength division multiplexer (WDM [43]). By stretching the coupling region of these devices it was shown that it is possible to effectively tune their spectral characteristics over ranges exceeding 15 nm without additional loss. Therefore, it is feasible to control the spectral function of the WDM in order to keep its relative position to the signature of the FBG when this is acted by the measurand, which means that such control signal turns out to be proportional to the resonant FBG shift.

To demonstrate this concept, the setup shown in Figure 9 was implemented. The WDM was fabricated by heating two fibers over a length of 3.0 mm and elongating

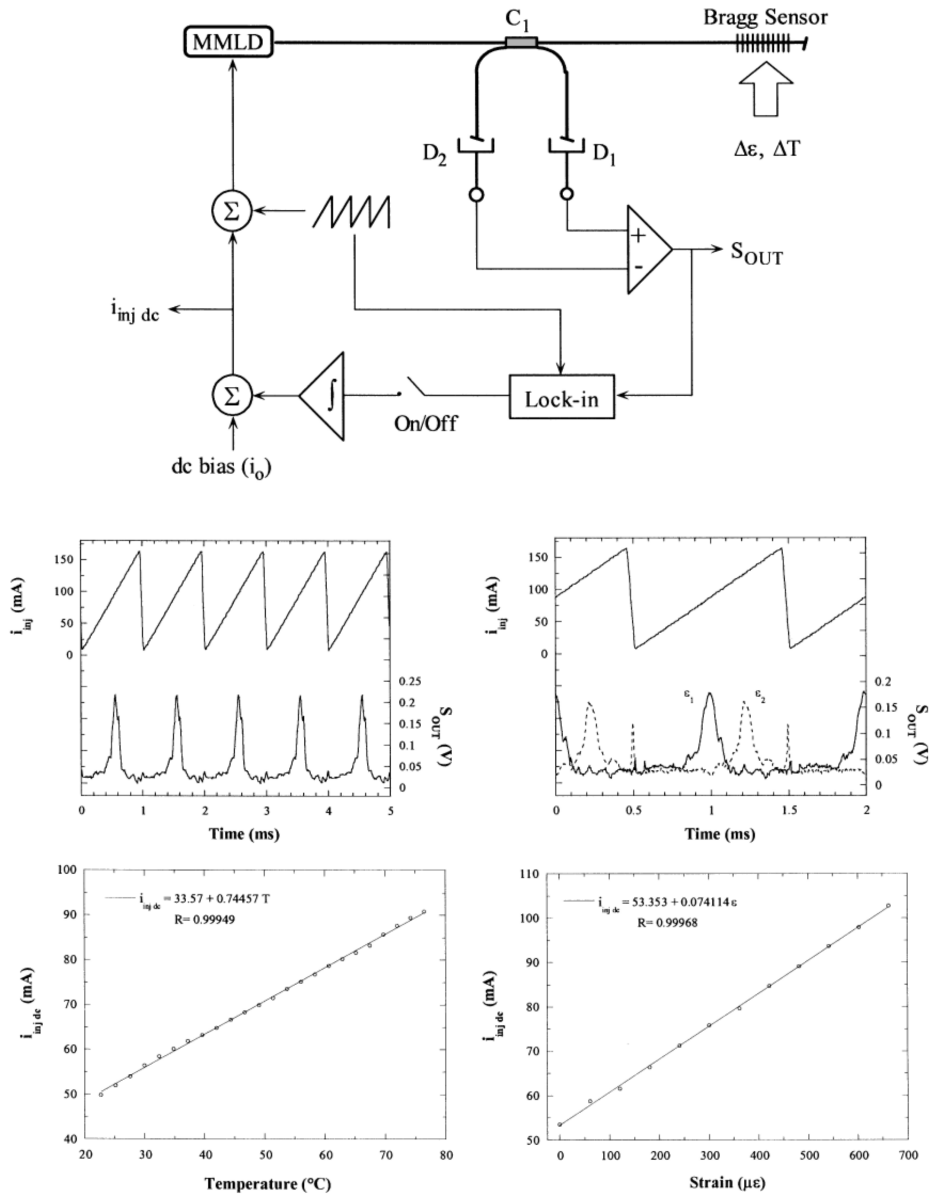

Figure 8. Experimental setup for FBG interrogation based on the sawtooth modulation of a multimode laser diode (top); sawtooth waveform applied to the laser diode and corresponding output carrier (middle left); demonstration of the effect on the output carrier when the strain applied to the sensor head changes by $\varepsilon_2 - \varepsilon_1 = 233\ \mu\varepsilon$ (middle right); system response to temperature and strain changes (from [39]).

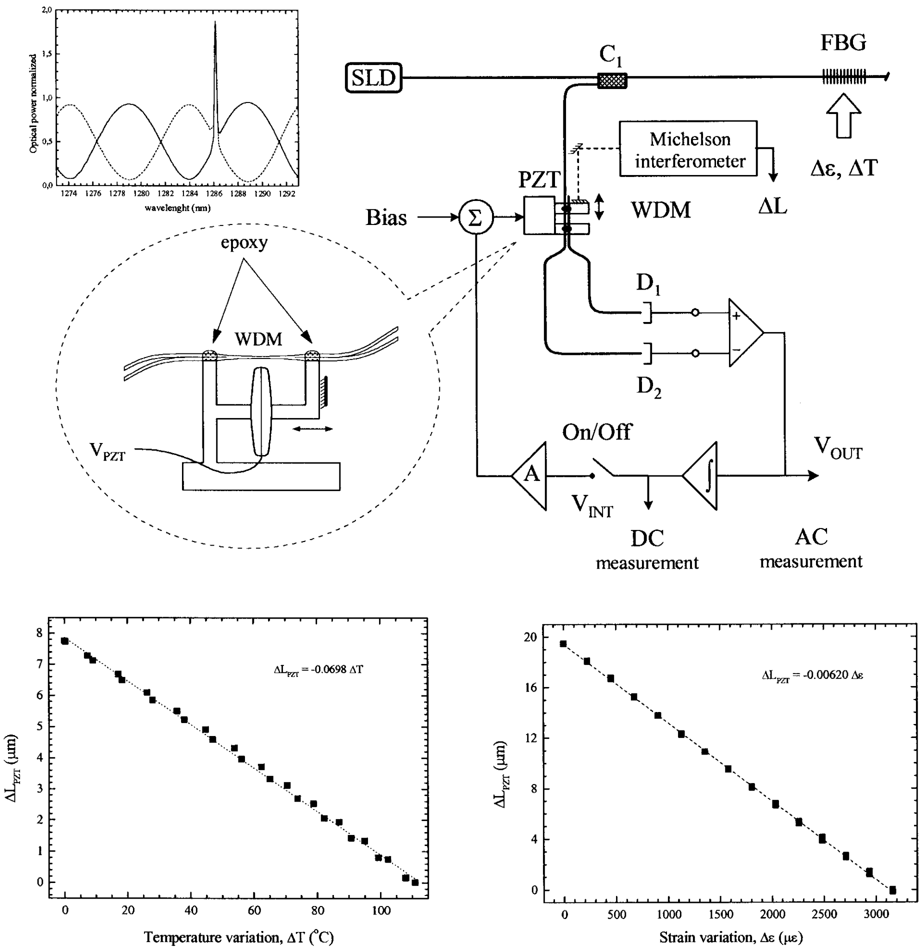

Figure 9. Demodulation of FBG sensors based on active control of the spectral response of a WDM. Experimental setup (top, inset left: relative position of the WDM and FBG spectral transfer functions; inset middle: detail of the WDM stretching mount); system response to temperature and strain changes (from [43]).

them by 25.5 mm, resulting in a device with a waist of 2.1 μm, a coupling length of $L = 9.6$ mm and a spectral periodicity of 9.8 nm. The feedback signal is applied to the PZT transducer used to stretch the WDM structure in order to keep the FBG signature tuned to the 3-dB point (Figure 9). The WDM tunability was measured to be $\Delta\lambda_{3\text{ dB}}/\Delta L = -0.17$ nm/μm.

This interrogation concept was applied to sensor readout when the FBG was subjected to temperature and strain changes. The obtained values are also shown in Figure 9. The resolutions achieved were, respectively, 0.2°C/$\sqrt{\text{Hz}}$ and 2.1 $\mu\varepsilon/\sqrt{\text{Hz}}$. These values can be substantially improved or relaxed by acting on the spectral period of the WDM, which also depends on the required measurement range and the level of feedback control signal that can be generated by the system to keep it locked.

Multi-Parameter Measurement Techniques

The simultaneous measurement of several parameters is an important topic, not only because, in general, it permits minimizing the complexity, size, and cost of a measurement system, but also because it fulfills the need to perform parameter discrimination in situations where cross-sensitivity is a crucial issue. As an example of this situation, the measurement of slowly varying strain is an important application of optical fiber sensors, but such measurement can be severely corrupted by the temperature cross-sensitivity, a situation that implies the need to independently measure these two parameters. The simplest way of measuring strain and temperature is to use physically separate sensing elements, where the first one is isolated from strain and experiences only temperature changes, and the second one is actuated by both strain and temperature. Provided the two sensing elements are at the same temperature, the output from the first sensor can be used to derive a temperature-corrected strain value from the second sensor. Various dual sensing element arrangements have been used, including serial deployment of in-fiber Bragg gratings or various forms of common-mode rejection. However, where sensors must be embedded with minimum intrusion in the measurement volume, the use of a second sensing element is not feasible. In these situations, strain and temperature measurement (or sets of other measurands) must be performed by a single sensing element [10, 45].

This issue has been the focus of intensive research worldwide and also in Portugal, as is clear from the review on this subject presented elsewhere in this journal.

Ferreira et al. [46, 47] presented a concept for simultaneous measurement of displacement and temperature based on the combination of a Fabry-Pérot cavity and an FBG. Simultaneous measurement of strain and temperature was achieved in different ways, such as the use of FBGs written in germanosilicate and boron-codoped germanosilicate fibers [48, 49], exploring the different temperature sensitivities of the two gratings resulting from a single writing step in a bow-tie hi-bi fiber [50], considering a sampled FBG associated with the combination of a FBG and a long period grating [51], and combining different types of FBGs [52]. The fabrication of gratings in a D-type hi-bi fiber permitted obtaining a temperature- and strain-insensitive bend sensor [53]. Also, a miniaturized sensing head constituted by three FBGs provided the conditions for the simultaneous determination of curvature, plane of curvature, and temperature [54]. A concept based on the utilization of chirped gratings was applied in an intensity-referenced, temperature-independent sensing head for measurement of curvature [55]. In the context of chemical sensing, etching of the FBG host fiber allowed the implementation of a sensing head with the capability of simultaneous measurement of refractive index and temperature [56].

Figure 10 illustrates one concept for simultaneous measurement of temperature and strain [57], which is based on the combination of two Bragg gratings, written in different fibers (SMF28, 3 mol% of GeO_2; Fibrecore PS 1500, 10 mol% of GeO_2, 14–18 mol% of B_2O_3) and with different reflectivities, to form a single signature with a stepped reflection spectral profile. The peak wavelength shift ($\Delta\lambda_{peak}$) and the spectral width at 6 dB ($SW_{6\,dB}$) of the stepped FBG structure were measured for different values of temperature and applied strain. The former ($\Delta\lambda_{peak}$) corresponds to the response of the B/Ge-doped fiber, while the latter ($SW_{6\,dB}$) corresponds to the combined response of both types of fibers under applied strain and/or temperature. Linear dependences of these parameters with temperature and strain were observed with slopes that permitted writing a system of two independent equations on ΔT and $\Delta\varepsilon$, from where it was possible to calculate these values through measurements of $\Delta\lambda_{peak}$ and $SW_{6\,dB}$. The achieved

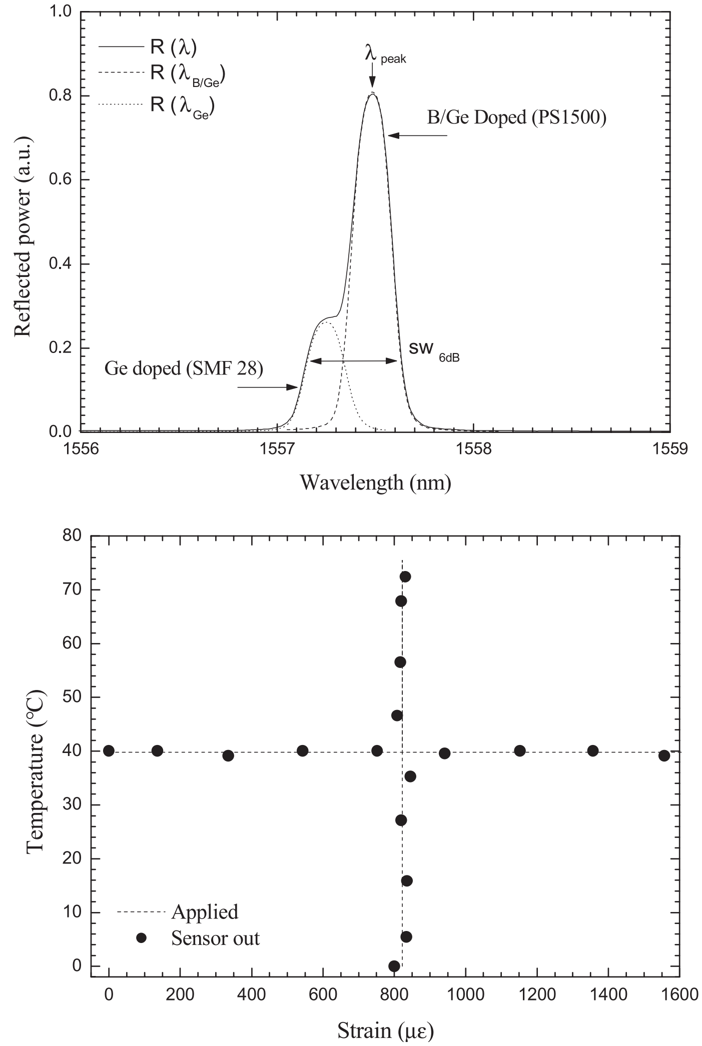

Figure 10. Stepped spectral profile as reflected by the FBG arrangement (left); sensor output as determined by the matrix equation for applied strain at constant temperature and temperature variation at constant strain (right) (from [57]).

resolutions can be obtained from the diagram shown in Figure 10, which were $0.7°C/\sqrt{Hz}$ and $\pm 2.6\ \mu\varepsilon/\sqrt{Hz}$.

Optical Current Sensors

The measurement of certain parameters in specific environments has been central in the development of fiber optic sensing technology. The fiber hydrophone for detection of objects in deep sea (based on Mach-Zehnder interferometers), the fiber gyroscope (relying on the Sagnac interferometer), and the electric current fiber meter (based on the magneto-optic effect) are in the top of this list [10]. Focusing on the measurement of electric current intensity in high-voltage environments, optical fiber–based solutions experienced considerable development over the last twenty years. Due to the intrinsic dielectric characteristics of the optical sensors, the need for insulation is greatly reduced. On the other hand, the magneto-optic effect, in which most configurations are based, has a constant linear response over a wide range of frequencies and, unlike effects employed in conventional sensors, presents no hysteresis or saturation effects for practical fields. Fiber or bulk closed-loop configurations, illuminated by optical fiber–guided radiation, are especially attractive because their closed optical path ensures immunity to external magnetic fields, which permits univocal current measurement [58].

This potential also triggered the R&D of this type of sensors in Portugal. A hybrid configuration, in which the secondary coil of a current transformer was adequately connected to a piezoelectric transducer with an FBG attached to it, resulting in a sensing head with Bragg wavelength shift proportional to the electric current, was developed and successfully tested in real conditions. Cavaleiro et al. [59] demonstrated another electric current concept based on a metal-coated FBG coupled to a standard current transformer. This structure uses the temperature-induced Bragg wavelength change that occurs when the electric current flows through a thin conductive coating on the surface of a short length of fiber where the FBG is located. In a measurement range up to 400 Å (rms value in the primary coil of the transformer), a resolution ±2 mA was reported. Due to the limited bandwidth of the sensor (≈2 Hz), its response was proportional to the rms value of the square of the current intensity. However, it was indicated that the frequency response could be increased up to tens of kilohertz by using a sputtering technique to produce a thinner and more uniform layer of metal over the FBG.

A different approach for current metering based on a bulk interferometric configuration was proposed by Jorge et al. [60]. The measurand information appears as a phase modulation of a frequency carrier; in this way, the sensor transfer function is independent of optical power fluctuations and has true linear dependence on the current intensity. The sensing head, represented in Figure 11, is a Mach-Zehnder interferometer with an additional reciprocal loop. The square-shaped loop, which works as a Sagnac interferometer, is built with low linear birefringence SF57 glass prisms. In order for the beam to remain confined within this loop, internal reflections are needed at the corners. To avoid unwanted phase terms, the technique of double reflections with complementary effects in each corner was used [61]. Due to the circular birefringence induced in the square loop by the magnetic field resulting from the electric current to be measured, an optical phase difference is introduced between the two orthogonal circular modes propagating in the Sagnac loop. Modulating the injection current of the laser diode with a sawtooth waveform of precise amplitude, a pseudo-heterodyne carrier is generated in the first interferometer (Mach-Zehnder), with its phase modulated by the electric current that propagates through the second interferometer (Sagnac). In fact, the authors showed that signals S_1 and S_r in Figure 11 are given by:

$$\begin{aligned} S_1 &= A[1 + \cos(\omega t + 2\theta L + \phi_0)] \\ S_r &= 2A[1 + \cos(\omega t + \phi_0)] \end{aligned} \tag{2}$$

where A is a constant proportional to the optical power injected into the sensing head, ω is the angular frequency of the sawtooth modulation, ϕ_0 is the quasi-static phase of the Mach-Zehnder interferometer, θ is the Faraday rotation per unit length (proportional to the electric current to be measured) and L is the total interaction length. Synchronous detection of S_1 relative to S_r gives the required measurand information, not corrupted

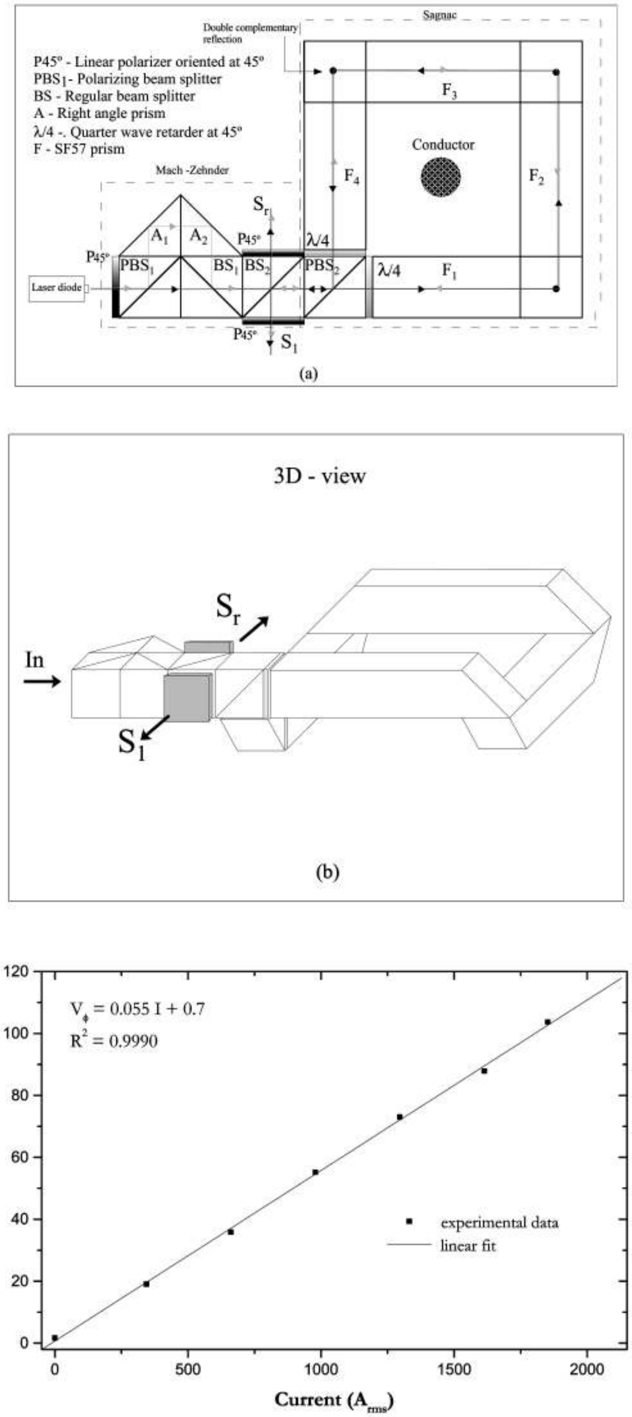

Figure 11. Interferometric sensing head for electric current metering (a); 3D view (b); system response to applied current (c) (from [60]).

by optical power fluctuations and intrinsically insensitive to reciprocal effects, like those induced by mechanical vibrations or temperature fluctuations.

Figure 11c shows an experiment on this system's response to applied current. Its sensitivity was calculated to be 1 kÅ^{-1} (rms), and the measured value was 1.7 kÅ^{-1} (rms). The resolution to current measurement was 17 Å_{rms} $\text{Hz}^{-1/2}$, a value essentially determined by laser diode–induced noise.

Sensor Multiplexing

In applications where sensing arrays are needed, multiplexing of fiber sensors will result in significant cost savings due to the reduction in the number of required light sources, detectors, and fiber transmission lines. A number of different approaches to sensor multiplexing have been reported, which may be described as forms of coherence, frequency, wavelength, and time division multiplexing [10].

Portuguese researchers and institutions have also been involved in this specific topic. Santos and Jackson [62] investigated the feasibility of time multiplexing of coherence addressed sensors using the spectral characteristics of multimode laser diodes. The study of topologies with particularly favorable characteristics to support time multiplexing of interferometric and intensity-based sensors was researched by Lobo Ribeiro et al. [63]. Later, time multiplexing was also considered in the context of FBG sensors interrogated using the filter spectral characteristics of specific optical sources [64]. Frequency multiplexing was also explored in the case of remote addressing of all-fiber Michelson interferometers deployed in a tree topology [65]. Coherence multiplexing was theoretically and experimentally investigated for coherence addressed polarimetric sensors in hi-bi fiber [66]. Wavelength-selective couplers were employed in the research of transparent networks for hybrid wavelength multiplexing of fiber Bragg grating and intensity-based fiber sensors [67, 68]. More recently, Baptista et al. [69] demonstrated FBG-assisted wavelength multiplexing of self-referenced intensity sensors.

In general, multiplexing involves the concepts of network topology, sensor addressing, and sensor interrogation. These concepts are frequently not independent, which means that the choice of one implies the selection of the other two. There are other relevant features conditioning the feasible configurations in a specific application. As an example, the integration of interferometric and intensity-based sensors turns problematic the utilization of reflective networks, since intensity sensors are normally implemented in multimode fiber, which implies the need for the return fiber bus to be also multimode. This constraint demands the utilization of a transmissive type network.

Lobo Ribeiro et al. [63] studied a topology with interesting characteristics for a fiber-sensing transmissive network referred to as the progressive ladder topology (PLT), which is illustrated in Figure 12a. For purpose of comparison, Figure 12b depicts the well-known transmissive ladder topology (TLT), which is probably the one that has been more utilized in transmissive networks suporting interferometric and intensity sensors. For simplicity, it is assumed that the transmissivity of each sensor is unitary, and that there are N sensors in the ladder placed in the rungs that are numbered from 1 through N. The fractional power transferred between the two fibers in coupler i is k_i, and $(1 - k_i)$ is the power that passes straight through. The crucial criterion for system design is to ensure that each sensor returns the same average optical power (I_S) from each rung of the array to the detector; i.e., $I_S(i) = I_S(i + 1)$ for all i between 1 and $N - 1$. To fulfill this criterion for the PLT network, and considering a lossless system, it was shown that the coupling ratios of all couplers must be identical, with the exception of the first

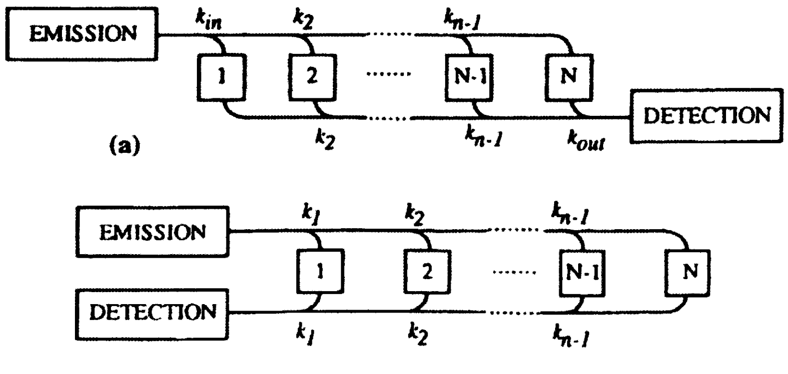

Figure 12. Fiber optic sensor network topologies: progressive ladder (a); transmissive ladder (b) (from [63]).

and last couplers, which occupy an asymmetric position in the network. This property is highly desirable because it avoids coupler tailoring along the network, which has implications in terms of system cost and, most important, facilitates the maintenance and repair procedures.

In a real system, it is necessary to consider the losses on the fibers, splices, couplers, and so on, which can be lumped together in the couplers, giving a total power attenuation factor of $(1 - \beta)$ and $(1 - \gamma)$ each time the light crosses a coupler in the input and output buses, respectively. Figure 13a shows the results for the coupler power ratios (k_i) as a function of their locations in the ladder, considering a network with 10 sensors, illuminated with 1300 nm radiation, and total power attenuation factors of $\beta = 0.84$ and $\gamma = 0.93$ (which means lumped losses of 0.75 dB and 0.3 dB, respectively). Not considering the special case of k_{in} and k_{out}, for the PLT system it can be observed from Figure 13a that the spread of values is relatively small, in strong contrast with the TLT case. Therefore, the PLT is an intrinsically balanced configuration, which is a highly desirable characteristic due to the reasons already mentioned. Figure 13b shows the behavior of the configurations PLT and TLT from the viewpoint of the sensor-returned average optical power as a function of the number of sensors. From these results, it turns out that the PLT configuration is also favorable in terms of power budget, with the corresponding positive implications in terms of sensor sensitivity.

Coherence multiplexing of optical fiber sensors is a conceptually neat technique, which permits addressing sensors distributed in a network and performing demodulation of signals induced on them by several physical measurands [70]. Sensor interrogation can be realized with a large dynamic range, and the sensor status can be recovered every time the system is turned on, which is a unique characteristic of this multiplexing concept. Its most important limitations are the large level of phase noise generated in the system (which is a consequence of the existence of multiple paths from the optical source to the detector) and, for implementation of the coherence addressing scheme, the need to have distinct path imbalances for the various sensors. The first limitation implies a reduction in the sensitivity of the sensors, while the second one imposes the properties of the sensors to be a function of their position in the network. The level of phase noise can be reduced by utilizing optical sources with low coherence (for example, SLDs). In this case, the path imbalance of the sensors can be very small, and this makes it attractive to perform

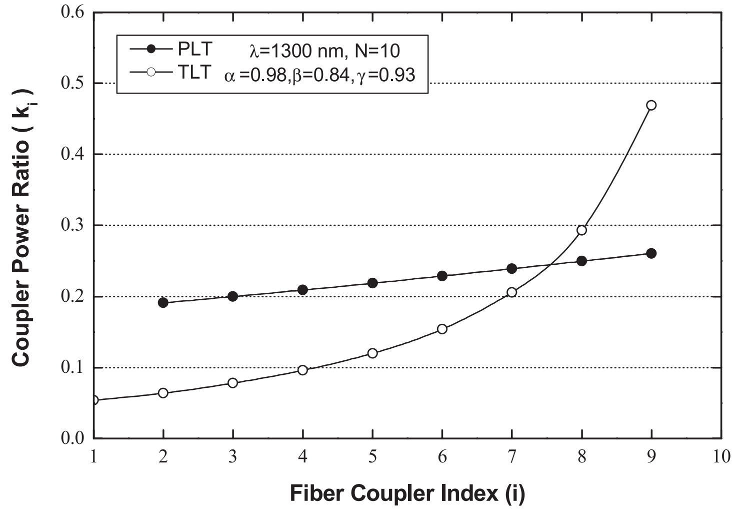

(a)

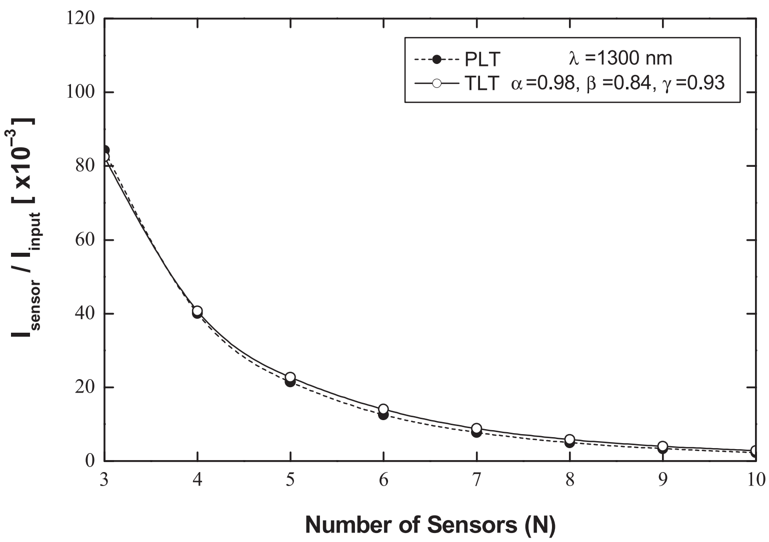

(b)

Figure 13. (a) Power ratio of the couplers as a function of their location in the array for the PLT and TLT topologies ($N = 10$, for a real system operating at 1300 nm); (b) averaged returned optical power per sensor (normalized by the input power) (from [63]).

coherence multiplexing of polarimetric sensors [71]. Figure 14 shows a multiplexing configuration of this type that was studied by Santos and Leite [66].

Radiation from a low-coherence optical source is injected into one of the eigenmodes (fast mode in the scheme of Figure 14) of a section of optical fiber with high birefringence (hi-bi fiber). At points A_i, $i = 1, 2, \ldots, N, N + 1$, where N is the number of sensors, radiation is coupled to the fast and slow modes of the next fiber section. This is done through the rotation, by an angle α, of the eigenaxis of the $i + 1$th section of fiber,

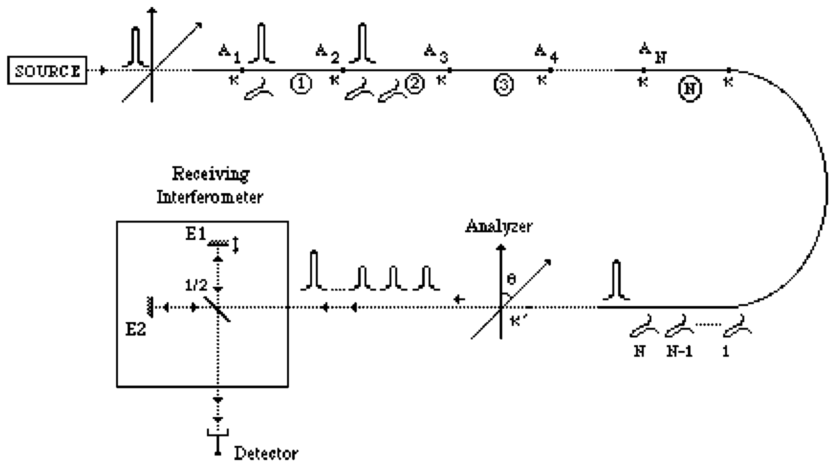

Figure 14. Coherence multiplexing of a series array of polarimetric sensors (only a fraction of the waves present, represented as pulses, are shown in the figure) (from [66]).

relative to the eigenaxis of the ith section. The power coupling factor of the radiation that propagates in the fast mode of section i to the slow mode of section $i+1$ (or vice versa) is, therefore, $\kappa = \text{sen}^2\alpha$. The sensor i is constituted by the fiber section between the coupling points A_i and A_{i+1}, its extension being sufficient to ensure that the radiation that propagates in its two eigenmodes (from point A_i) is mutually incoherent at the coupling point A_{i+1} (therefore avoiding interference that would occur if this condition were not satisfied). To simplify, it is assumed that the coupling factor is the same at all coupling points. The radiation that exits the end of the last fiber section crosses an analyzer with optical axis making an angle θ with the fast axis of the fiber ($\kappa' = \text{sen}^2\theta$). Then, the transmitted radiation is injected into the receiving interferometer (bulk Michelson). Its path imbalance is variable, thus making possible the successive tuning of the various sensing interferometers. By fulfilling the condition that the global path imbalance of the sensing and receiving interferometers corresponds to a quadrature point of the system transfer function, homodyne detection can be implemented. Heterodyne detection can also be achieved by applying a sawtooth waveform with proper amplitude to mirror E_2 of the receiving interferometer.

The signal-to-noise ratio is optimized if the optical axis of the analyzer makes an angle of 45° with the eigenaxis of the last section of fiber ($\kappa' = 1/2$). On the other hand, the minimum sensor phase signal detectable ($\phi_{s|source}$, for a unitary signal-to-noise ratio) is, in the large majority of the cases, determined by source-induced noise. If the optical source has Gaussian characteristics mapped into a coherence time τ_c, then it can be shown that this minimum phase, when normalized to the system detection bandwith, B, is only a function of the coupling factor κ, being given by [66]:

$$\frac{\phi_{s|source}}{\sqrt{B}} = \left\{ \frac{3\tau_c \left[\frac{3}{2} - 2\left(\kappa - \frac{1}{2}\right)^2 \right]^{N+1}}{2\kappa^2(1-\kappa)^2} \right\}^{1/2} \tag{3}$$

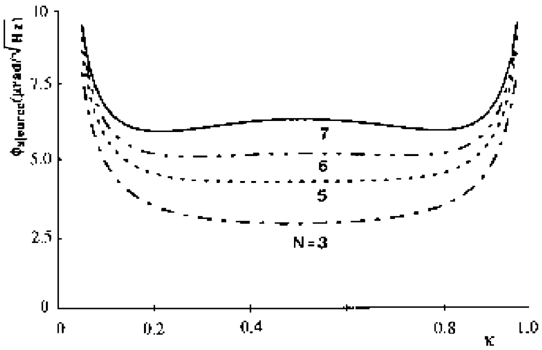

(a)

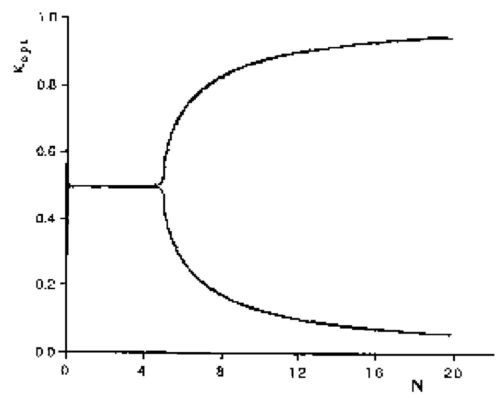

(b)

Figure 15. Minimum detectable phase, as a function of κ, when only source-induced noise is considered (a); values of κ that minimize $\phi_{s|source}$ (b) (from [66]).

For the case of $L_C = c\tau_c = 20$ μm, Figure 15 shows $\phi_{s|source}$ versus κ. From this figure, it is clear that the value of κ that minimizes $\phi_{s|source}$ is a function of N.

Applications and Field Trials

After an initial phase of the R&D in fiber sensing, as summarized in previous sections, the results obtained triggered a certain number of initiatives involving Portuguese companies toward the use of this technology in specific applications. The first of these initiatives occurred in 1997 and involved real-time monitoring of the temperature of electric power cables using FBGs to support an optimization of electric power distribution networks. The problem of conventional technology replacement in the context of electric current metering and current transients in high-voltage environments was also addressed. Two optical fiber–based configurations were developed that underwent field tests with appreciable performance.

Another area where optical fiber sensors, particularly those based on fiber Bragg gratings, offer a high potential as replacement technology is in structure monitoring, mainly in civil engineering. Indeed, Bragg gratings can directly replace electric strain gauges, surpassing the limitations of these devices, as their calibration is absolute (optical wavelength), they are completely immune to EMI/RFI, and they are intrinsically amenable to multiplexing. Consequently, several projects were implemented in the context of civil engineering, with particular focus on the monitoring of concrete bridges and also of historic iron bridges in the city of Porto. The outcome of such actions was illustrative of the advantages of the fiber optic sensing technology relative to the conventional electric based monitoring solutions, and this stimulated the recent launch of a fiber-sensing spin-off devoted to the developement of fiber optic–based sensing systems (www.fibresensing.com). This technology was also tested with success in the context of composite material monitoring for smart structures.

Another initiative where fiber optic sensors were taken into the field was in the context of environmental monitoring. A project was set aiming to study the dynamics of Ria de Aveiro, an important Portuguese coastal lagoon. One of the required parameters to be monitored was the distribution of water temperature along the 12-km extension of the lagoon, from the connection to the sea up to the location where freshwater is delivered to the system by the feeding river. An optical cable incorporating fiber Bragg gratings was developed and installed. The interrogation equipment, installed in the location, is continuously acquiring data from the FBGs and delivering it to the remote sites of the institutions involved in the project for further processing and analysis. Figure 16 shows one example of the stream of data relative to water temperature measured by three FBGs of the cable.

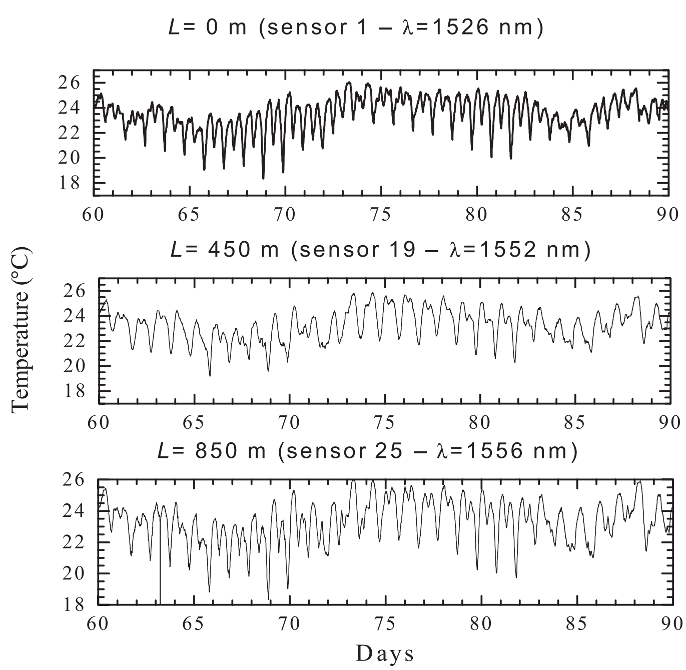

Figure 16. Daily variation of water temperature registered along a period of one month by some of the FBGs sensors installed in Ria de Aveiro lagoon ($L = 850$ m is closer to the sea).

Recently, FBG-based sensors have also been applied in clinical studies of the dynamics analysis of the mandible, aiming at the development of replacement prosthesis [72]. The quality of the results obtained clearly indicates the advantages of using this sensing technology in other biomechanics applications.

Concluding Remarks

Most of the fiber-sensing R&D activity performed in Portugal up to the present was directed toward the measurement of physical quantities (temperature, strain, pressure, vibration, displacement, etc.). Their detection, either single- or multi-point, required an approach simultaneously involving fiber optic technology for sensing head design and fabrication, signal processing, and multiplexing issues, among others. This orientation will surely be continued, not only by mastering sensing solutions already identified, but also by looking for new ones. In particular, special emphasis will be put on research of sensing heads exhibiting advanced characteristics, such as absence of cross-sensitivity to temperature, aging self-diagnostic, multiparameter detection, etc., and on sensor interrogation techniques with enhanced sensitivity, as well as multiplexing. Following this track, research work on fiber optic devices with complex spectral structure, possessing the degrees of freedom needed for advanced sensing, will be most relevant. Fiber Bragg gratings, long period gratings, fused biconical tapers/couplers, microstructured optical fibers, interferometers, and microcavities are examples of types of devices that, when properly designed and fabricated, considered either in single configuration or in combination, can be used to attain the required functionalities. Complementary to this approach, actions directed to field applications of the technology and the establishment of spin-off enterprises will be pursued.

A few years ago, it was considered that the basic conditions existed to expand the national R&D activity in fiber optic sensing to the chemical and biochemical fields. This is a huge world of demand and innovation, which is largely unexplored. There are many types of sensing technologies with potential to be applied in this domain, but none yet has an established position. Common to all of them, there is a need for an interface capable of transducing the measurand action into parameters intrinsic to the particular technology used. This interface must always have a chemical/biochemical component, which requires a strong interdisciplinary approach for its development. In this context, it is accepted that optical fiber technology, when combined with integrated optics, can provide biochemical sensing platforms with interesting characteristics, particularly in what concerns distributed sensing. This is a challenging R&D path to be pursued in the future.

Until recently, the fiber-sensing R&D activity in Portugal was essentially centerd in the city of Porto. However, the situation is changing fast and the University of Aveiro is increasingly engaged in the field. Other Portuguese R&D institutions will certainly be joining this effort, a guarantee of a healthy dynamics for the development of optical fiber–sensing technology in Portugal.

Acknowledgments

The authors would like to acknowledge the financial support, in the form of R&D contracts and fellowships, of Portuguese Research Council (Fundação para a Ciência e Tecnologia) and of the European Commission. Through the years those projects were instrumental to the establishment of the R&D activity in fiber optic sensing in Portugal.

References

1. Culshaw, B. 2004. Optical fiber sensor technologies: Opportunities and—perhaps—pitfalls. *J. Lightwave Technol*. 22(1):39–49.
2. Jackson, D. A. 1985. Monomode optical fibre interferometers for precision measurement. *Journal Physics E: Scientific Instruments* 18:981–1001.
3. Kersey, A. D., D. A. Jackson, and M. Corke. 1983. A simple fibre Fabry-Perot sensor. *Optical Communications* 45:71–75.
4. Berkoff, A. T., and A. D. Kersey. 1990. Interferometric fibre displacement/strain sensor based on source coherence synthesis. *Electronic Letters* 26:452–453.
5. Venkatesh, S., and W. V. Sorin. 1991. Fibre-tip displacement sensor using sinusoidal FM-based techniques. *Electronics Letters* 27:1652–1654.
6. Wright, O. B. 1991. Stabilized dual wavelength fiber-optic interferometer for vibration measurement. *Optics Letters* 16:56–58.
7. Murphy, K. A., M. F. Gunther, A. M. Vengsarkar, and R. O. Claus. 1991. Quadrature phase-shifted extrinsic Fabry-Perot optical fiber sensors. *Optics Letters* 16:273–275.
8. Santos, J. L., and D. A. Jackson. 1992. Passive demodulation of miniature fiber-optic based interferometric sensors using a time multiplexing technique. *Optics Letters* 16(15):1210–1212.
9. Santos, J. L., A. P. Leite, and D. A. Jackson. 1992. Optical fiber sensing with a low-finesse Fabry-Perot cavity. *Applied Optics* 31(34):7361–7366.
10. López-Higuera, J. M., ed. *Handbook of optical fibre sensing technology*. Chichester, UK: John Wiley, 2002.
11. Dahlem, M., J. L. Santos, L. A. Ferreira, and F. M. Araújo. 2001. Passive interrogation of low-finesse Fabry-Pérot cavities using fiber Bragg gratings. *IEEE Photonics Technology Letters* 13(9):990–992.
12. Heredero, R. L., S. Martin, R. F. De Caleya, A. B. Lobo Ribeiro, F. M. Araújo, L. A. Ferreira, J. L. Santos, and H. Guerrero. 2002. A study of the optical properties of photopolymer Fabry-Pérot microcavities by a dual-wavelength fibre optic architecture. *Journal of Measurement Science and Technology* 13:1094–1099.
13. Jáuregui Misas, C., F. M. Araújo, L. A. Ferreira, J. L. Santos, and J. M. López-Higuera. 2001. Interrogation of low-finesse Fabry-Pérot cavities based on modulation of the transfer function of a wavelength division multiplexer. *Journal Lightwave Technology* 19(5):673–681.
14. Jackson, D. A., and J. Jones. 1986. Fibre optic sensors. *Optica Acta* 33(12):1469–1503.
15. Kersey, A. D., M. J. Marrone, and A. Dandridge. 1990. Analysis of input-polarization-induced phase noise in interferometric fiber-optic sensors and its reduction using polarization scrambling. *Journal Lightwave Technology* 8(6):838–845.
16. Kersey, A. D., M. J. Marrone, A. Dandridge, and A. B. Tveten. 1988. Optimization and stabilization of visibility in interferometric fiber-optic sensors using input-polarization control. *Journal Lightwave Technology* 6(10):1599–1609.
17. Kersey, A. D., and M. J. Marrone. 1990. Quadrature phase sampling of a fibre interferometer by input-polarisation switching. *Electronics Letters* 26(11):686–688.
18. Kersey, A. D., M. J. Marrone, and M. A. Davis. 1991. Polarisation-insensitive fibre optic Michelson interferometer. *Electronics Letters* 27(6):518–520.
19. Pistoni, N. C., and M. Martinelli. 1991. Polarisation noise suppression in retracing Optical fibre circuits. *Optics Letters* 16(10):711–713.
20. Gauthier, R. R., F. Farahi, and N. Dahi. 1994. Down-lead sensitivity in coherence multiplexed sensing systems. *Optics Letters* 19(2):138–141.
21. Ferreira, L. A., J. L. Santos, and F. Farahi. 1995b. Polarization insensitive fibre-optic white-light interferometry. *Optics Communications* 114:386–392.
22. Ferreira, L. A., J. L. Santos, and F. Farahi. 1995a. Polarization-induced noise in a fiber-optic Michelson interferometer with Faraday rotator mirror elements. *Applied Optics* 34(28):6399–6402.
23. Murtaza, G., and J. M. Senior. 1994. Referenced intensity-based optical fibre sensors. *International Journal of Optoelectronics* 9:339–348.

24. Baptista, J. M., P. M. Cavaleiro, and J. L. Santos. 1995. Self-referencing intensity based Q-type fibre optic sensor. *International Journal Optoelectronics* 10(2):105–113.
25. Baptista, J. M., P. M. Cavaleiro, and J. L. Santos. 1996. Self-referencing resonant fibre optic intensity sensor based on a Mach-Zehnder topology. *Review Scientific Instruments* 67(11): 3788–3795.
26. Baptista, J. M., J. L. Santos, and A. S. Lage. 2000a. Mach-Zehnder and Michelson topologies for self-referencing fibre optic intensity sensors. *Optical Engineering* 39(6):1636–1642.
27. Baptista, J. M., J. L. Santos, and A. S. Lage. 2000b. Self-referenced fibre optic intensity sensor based on a multiple beam Sagnac topology. *Optics Communications* 181:287–294.
28. Baptista, J. M., O. Frazão, L. A. Ferreira, F. M. Araújo, J. L. Santos, and A. S. Lage. 2003. Load cell for structural monitoring based on a microbend self-referenced fibre optic intensity sensor. *Sixteenth Annual Meeting of the IEEE Lasers & Electro-Optics Society*, 93–94.
29. Cavaleiro, P. M., A. B. Lobo Ribeiro, and J. L. Santos. 1995. Referencing technique for intensity-based sensors using fibre optic Bragg gratings. *Electronics Letters* 31(5):392–394.
30. Abad, S., M. López-Amo, F. M. Araújo, L. A. Ferreira, and J. L. Santos. 2002. Fibre Bragg grating based self-referencing technique for wavelength-multiplexed intensity sensors. *Optics Letters* 27:222–224.
31. Araújo, F. M., E. Joanni, M. J. Marques, and O. G. Okhotnikov. 1998. Dynamics of IR absorption caused by hydroxyl groups and its effect on refractive index evolution in UV exposed hydrogen loaded GeO2 doped fibres. *Applied Physics Letters* 72(24):3109–3115.
32. Lobo Ribeiro, A. B., L. A. Ferreira, M. Tsvetkov, and J. L. Santos. 1996. All-fibre interrogation technique for fibre Bragg sensors using a biconical fibre filter. *Electronics Letters* 32(4):382–383.
33. Ferreira, L. A., and J. L. Santos. 1996. Demodulation scheme for fibre Bragg sensors based on source spectral characteristics. *Pure and Applied Optics* 5:257–261.
34. Abad, A., F. M. Araújo, L. A. Ferreira, J. L. Santos, and M. López-Amo. 2003b. Interrogation of wavelength multiplexed fiber Bragg gratings using spectral filtering and amplitude-to-phase optical conversion. *Journal of Lightwave Technology* 21(1):127.
35. Romero R., O. Frazão, P. V. S. Marques, H. M. Salgado, and J. L. Santos. 2003. Fibre Bragg grating interrogation technique based on a chirp grating written in an erbium doped fibre. *Journal of Measurement Science and Technology* 14:1993.
36. Lobo Ribeiro, A. B., L. A. Ferreira, J. L. Santos, and D. A. Jackson. 1997. Analysis of the reflective matched fibre Bragg grating sensing interrogation scheme. *Applied Optics* 36(4):934–939.
37. Ferreira, L. A., J. L. Santos, and F. Farahi. 1997. Pseudo-heterodyne demodulation technique for fibre Bragg grating sensors using two matched gratings. *IEEE Photonics Technology Letters* 9(4):487–489.
38. Jorge, P. A. S., L. A. Ferreira, and J. L. Santos. 2000. Analysis of the flyback effects on the serrodyne interferometric demodulation of fiber optic Bragg grating sensors. *Optical Engineering* 39(5):1399–1404.
39. Ferreira, L. A., E. V. Diatzikis, J. L. Santos, and F. Farahi. 1998. Frequency modulated multimode laser diode for fibre Bragg grating sensors. *Journal of Lightwave Technology* 16(9): 1620–1630.
40. Ferreira, L. A., J. L. Santos, E. V. Diatzikis, and F. Farahi. 1999. Demodulation of fibre Bragg gratings sensors based on dynamic tuning of a multimode laser diode. *Applied Optics* 38(22):4751–4759.
41. Ferreira, L. A., E. V. Diatzikis, P. J. Moreira, J. L. Santos, and F. Farahi. 2000. Application of multimode laser diodes in the interrogation of fiber Bragg grating sensors. *Optical Fiber Technology* 6:365–387.
42. Moreira, P. J., L. A. Ferreira, J. L. Santos, and F. Farahi. 1999. Dynamic range enhancement in fibre Bragg grating sensors using a multimode laser diode. *IEEE Photonics Technology Letters* 11(6):703–705.
43. Araújo, F. M., L. A. Ferreira, J. L. Santos, and F. Farahi. 1998. Demodulation scheme for fibre Bragg grating sensors based on active control of the spectral response of a wavelength division multiplexer. *Applied Optics* 37(34):7940–7946.

44. Jáuregui Misas, C., F. M. Araújo, L. A. Ferreira, J. L. Santos, and J. M. López-Higuera. 2000. Fiber Bragg sensors interrogation based on carrier generation by modulating the coupling length of a wavelength-division multiplexer. *IEEE Selected Topics in Quantum Electronics* 6(5):750–755.
45. Jones, J. D. C. 1997. Review of fiber sensor techniques for temperature-strain discrimination. *Twelfth International Conference on Optical Fiber Sensors*, 36–39.
46. Ferreira, L. A., A. B. Lobo Ribeiro, J. L. Santos, and F. Farahi. 1996. Simultaneous measurement of displacement and temperature using a low finesse cavity and a fiber Bragg grating. *IEEE Photonics Technology Letters* 8(11):1519–1521.
47. Ferreira, L. A., A. B. Lobo Ribeiro, J. L. Santos, and F. Farahi. 1998. Simultaneous displacement and temperature sensing using a white light interrogated low finesse cavity in line with a fiber Bragg grating. *Smart Materials and Structures* 7:189–198.
48. Cavaleiro, P. M., F. M. Araújo, L. A. Ferreira, J. L. Santos, and F. Farahi. 1999. Simultaneous measurement of strain and temperature using Bragg gratings written in germanosilicate and boron-codoped germanosilicate fibers. *IEEE Photonics Technology Letters* 11(12):1635–1637.
49. Frazão, O., and J. L. Santos. 2004. Simultaneous measurement of strain and temperature using a Bragg grating structure written in germanosilicate fibres. *Journal Optics A: Pure Applied Optics* 6:553.
50. Ferreira, L. A., F. M. Araújo, J. L. Santos, and F. Farahi. 2000. Simultaneous measurement of strain and temperature using interferometrically interrogated fiber Bragg grating sensors. *Optical Engineering* 39(8):2226–2234.
51. Frazão, O., R. Romero, G. Rego, P. V. S. Marques, H. M. Salgado, and J. L. Santos. 2002. Sampled fibre Bragg grating sensors for simultaneous strain and temperature measurement. *Electronics Letters* 38(14):693–695.
52. Frazão, O., M. J. N. Lima, and J. L. Santos. 2003. Simultaneous measurement of temperature and strain using type I and type IIA fiber Bragg gratings. *Journal of Optics A: Pure and Applied Optics* 5:183.
53. Araújo, F. M., L. A. Ferreira, J. L. Santos, and F. Farahi. 2001. Temperature and strain insensitive bending measurements with D-type fibre Bragg gratings. *Measurement Science and Technology* 12:829–833.
54. Araújo, F. M., L. A. Ferreira, and J. L. Santos. 2002. Simultaneous determination of curvature, plane of curvature, and temperature by use of a miniaturized sensing head based on fiber Bragg gratings. *Applied Optics* 41(13):2401–2407.
55. Romero, R., O. Frazão, D. A. Pereira, and H. M. Salgado. 2004. Intensity-referenced temperature-independent curvature sensing concept based on chirped gratings embedded in a composite laminate. *Second Workshop on Optical Fibre Sensors*, 164–167.
56. Pereira, D. A., O. Frazão, and J. L. Santos. 2004. Fiber Bragg grating sensing system for simultaneous measurement of salinity and temperature. *Optical Engineering* 43(2):299–304.
57. Frazão, O., R. Romero, F. M. Araújo, L. A. Ferreira, and J. L. Santos. 2004. Simultaneous measurement of temperature and strain using a step spectrum profile Bragg grating arrangement. *Second Workshop on Optical Fibre Sensors*, 36–39.
58. Ning, Y. N., Z. P. Wang, A. W. Palmer, and K. T. V. Gratan. 1995. Recent progress in optical current sensing techniques. *Review of Scientific Instruments* 5:3097–3111.
59. Cavaleiro, P. M., F. M. Araújo, and A. B. Lobo Ribeiro. 1998. Metal-coated fibre Bragg grating sensor for electric current metering. *Electronics Letters* 34:1133–1135.
60. Jorge, P. A. S., P. Caldas, L. A. Ferreira, A. B. Lobo Ribeiro, J. L. Santos, and F. Farahi. 2002. Electrical current metering with a dual interferometric configuration and serrodyne signal processing. *Measurement Science and Technology* 13:533–538.
61. Ning, Y. N., B. C. B. Chu, and D. A. Jackson. 1991. Miniature Faraday current sensor based on multiple critical angle reflections in a bulk-optic ring. *Optics Letters* 16:1996–1998.
62. Santos, J. L., and D. A. Jackson. 1991. Time multiplexing of coherence tuned optical fibre sensors based upon a multimode laser diode. *Optics Communications* 83:37–42.

63. Lobo Ribeiro, A. B., R. F. Caleya, and J. L. Santos. 1995. Progressive ladder network topology combining interferometric and intensity fibre-optic-based sensors. *Applied Optics* 34(28):6481–6488.
64. Ferreira, L. A., P. C. Dias, and J. L. Santos. 1997. Demodulation of two time-multiplexed fibre Bragg sensors using source spectral characteristics. *Pure and Applied Optics* 6:717–726.
65. Santos, J. L., F. Farahi, T. Newson, A. P. Leite, and D. A. Jackson. 1992. Frequency multiplexing of remote all-Fiber Michelson interferometers with lead insensitivity. *Journal of Lightwave Technology* 10(6):853–863.
66. Santos, J. L., and A. P. Leite. 1993. Multiplexing of polarimetric sensors addressed in coherence. *Ninth Internacional Conference on Optical Fibre Sensors*, 59–62.
67. Abad, S., F. M. Araújo, L. A. Ferreira, J. L. Santos, and M. Lopez-Amo. 2003c. Transparent network for hybrid multiplexing of fiber Bragg gratings and intensity-modulated fiber-optic sensors. *Applied Optics* 42(25):5040.
68. Abad, S., F. M. Araújo, L. A. Ferreira, J. L. Santos, and M. Lopez-Amo. 2003a. Comparative analysis of wavelength-multiplexed photonic-sensor networks using fused biconical WDMS. *IEEE Sensors Journal* 3(4):475.
69. Baptista, J. M., S. Abad, G. M. Rego, L. A. Ferreira, F. M. Araújo, and J. L. Santos. 2004. Wavelength multiplexing of frequency-based self-referenced fiber optic intensity sensors. *Optical Engineering* 43(3):702–707.
70. Cusmeroli, V., M. Martinelli, and P. Vavassor. 1989. Quasi-distributed single length polarimetric sensor. *Optics Letters* 14:1330–1332.
71. Farhadiroushan, M., and R. Youngquist. 1990. Polarimetric coherence multiplexing using high birefringence optical fiber sensors and short coherence sources. *Optics Letters* 15:786–788.
72. Silva, J. C. C., L. Carvalho, R. N. Nogueira, J. A. Simões, J. L. Pinto, and H. J. Kalinowski. 2004. FBG applied in dynamic analysis of an implanted cadaveric mandible. *Second Workshop on Optical Fibre Sensors*, 226–229.

Biographies

A. B. Lobo Ribeiro graduated in applied physics (optics and electronics) from the University of Porto, Portugal, in 1990. He received an M.Sc. in physics (applied optics) from the University of Kent, Canterbury, U.K. (1992), and a Ph.D. degree in physics from the University of Porto (1997) in the context of fiber optic sensor multiplexing networks. He is associate professor of the Faculty of Health Sciences of University Fernando Pessoa, Porto, Portugal. His actual research interests include fiber optic sensors and optical microdevices, biomedical optic sensors, distributed optical sensing, and nonlinear fiber optics. He is also a regular member of SPIE.

J. L. Santos graduated in applied physics (optics and electronics) from the University of Porto, Portugal, in 1983. In 1993 he was awarded a Ph.D. degree in physics from the same university for research in fiber optic sensing. He is an associate professor in the physics department of University of Porto and is in charge of the Optoelectronics and Electronic Systems Unit of INESC Porto. His main research interests are in the optical fiber sensing field. He is a member of OSA and SPIE.

J. M. Baptista graduated in electrical and computer engineering (telecommunications and computers) from the University of Porto, Portugal, in 1991. He received his M.Sc. in physics of laser communications from the University of Essex, Colchester, U.K. (1992), and a Ph.D. degree in electrical and computer engineering from the University of Porto (2002). Currently, he is teaching in the Polytechnic Institute of Porto and he is a researcher of Optoelectronics and Electronics Systems Unit of INESC, Porto. His research interests are in the areas of fiber optic sensors and optical communications. He is member of SPIE and IEEE.

L. A. Ferreira graduated in applied physics (optics and electronics) in 1991 and obtained an M.Sc. degree in optoelectronics and lasers in 1995, both from the University of Porto, Portugal. He received his Ph.D. degree in physics from the same university in 2000. Presently he is a senior researcher at the Telecommunications and Multimedia Unit of INESC, Porto. His main activity is related with optical communications and fiber optic sensing. He is also a co-founder of FibreSensing, an INESC Porto spin-off company developing fiber optic sensors and monitoring systems.

F. M. Araújo graduated in applied physics (optics and electronics) from the University of Porto, Portugal, in 1993. In 2000 he was awarded a Ph.D. degree in physics from the same university. Presently he is a senior researcher at the Telecommunications and Multimedia Unit of INESC, Porto. His main activity is related with optical communications and fiber optic sensing. He is also a co-founder of FibreSensing, an INESC Porto spin-off company developing fiber optic sensors and monitoring systems.

A. P. Leite graduated in electrical engineering from the University of Porto, Portugal, in 1973. In 1979 he was awarded a Ph.D. degree from University College London, Department of Electronic and Electric Engineering, for research in holographic optical elements. Appointed associate professor at the Department of Physics, University of Porto, in 1979, he has been involved since then in projects on optical communication, fibre sensors, and integrated optic devices in lithium niobate, III-V semiconductors, polymers, and glass. His current interests are in the field of integrated optics (glass and polymer devices, electro-optic, and rare-earth–doped devices), fiber sensors, and sensor networks.